Hindawi Publishing Corporation
Journal of Nanotechnology
Volume 2014, Article ID 285857, 7 pages
http://dx.doi.org/10.1155/2014/285857

Research Article

Noncovalent Attachment of PbS Quantum Dots to Single- and Multiwalled Carbon Nanotubes

Anirban Das,[1,2] Eric Hall,[1] and Chien M. Wai[1]

[1] *Department of Chemistry, University of Idaho, Renfrew Hall, Moscow, ID 83844, USA*
[2] *Center for Catalysis and Surface Science, Northwestern University, 2137 Tech Drive, Evanston, IL 60208-3000, USA*

Correspondence should be addressed to Anirban Das; anirban.das@northwestern.edu

Received 8 June 2013; Revised 31 January 2014; Accepted 1 February 2014; Published 10 March 2014

Academic Editor: Bobby G. Sumpter

Attachment of PbS quantum dots (QD) to single-walled carbon nanotubes (SWNT) and multiwalled carbon nanotubes (MWCNT) is described; wherein commercially obtained PbS-QD of size 2.7 nm, stabilized by oleic acid, are added to a suspension of single- or multiwalled carbon nanotubes (CNT) prefunctionalized noncovalently with 1,2-benzenedimethanethiol (1,2-BDMT) in ethanol. The aromatic part of 1,2-BDMT attaches to the CNT by π-π stacking interactions, noncovalently functionalizing the CNT. The thiol part of the 1,2-BDMT on the functionalized CNT replaces oleic acid on the surface of the QD facilitating the noncovalent attachment of the QD to the CNT. The composites were characterized by TEM and FTIR spectroscopy. Quenching of NIR fluorescence of the PbS-QD on attachment to the carbon nanotubes (CNT) was observed, indicating FRET from the QD to the CNT.

1. Introduction

PbS-QD of sizes smaller than 10 nm, by virtue of quantum confinement, absorb and emit energy in the near-IR (NIR) region of the electromagnetic spectrum, making them suitable for applications like harvesting solar energy [1], biological sensors [2], and telecommunications [3]. Due to the large exciton Bohr radii of PbS (20 nm) and PbSe (46 nm) [4], these semiconductor QD permit the largest quantum confinement among III-VI materials leading to intensification of size dependent properties that arise due to quantum confinement in nanomaterials. These and similar semiconducting QD when coupled with CNTs (carbon nanotubes) have been demonstrated to have a multitude of applications such as construction of electronic and photonic nanodevices including solar energy harvesters [5–8], biological imaging [9], and IR detectors [10, 11]. To be suitable for the above applications, these composites must demonstrate the phenomena of either energy transfer [12] or charge transfer [5] from the QD to CNT. These phenomena modify the optical properties of both the former and the latter [13]. One of the above properties, resonance energy transfer, is dependent on the distance between the particle and the nanotube (known as the Föster radius, typically a few nanometers [14]) as well as on the overlap of energy levels [12] between the former and the latter. As shall be discussed in detail in a later section of this report, the energy levels of PbS-QD of appropriate sizes overlap effectively with the energy levels of both SWNT [15] and MWCNT [16]. Thus if novel PbS-QD-CNT composites are synthesized where the semiconducting PbS-QD and the CNT are closer than the Föster radius, then these composites may be explored for increasing the efficiency of the existing devices and development of new applications. Here we report synthesis of PbS-QD-CNT composites where the quantum confined PbS-QD and the CNT, separated by a C–C–S bond, are within a few angstroms of each other. Further studies into optical and electronic properties of these composites may be carried out towards development of more efficient solar energy conversion devices [5] and other applications based on unique properties of these composites.

There are several reports of attachment of semiconductor QD to CNT as reviewed briefly below. Out of the two possible methods to attach QD to CNTs, covalent and noncovalent, the latter is preferred as the structure and hence the unique properties that arise due to the CNT's structure are preserved. Noncovalent attachment is especially significant for SWNT as they have a single sidewall and its covalent functionalization would lead to destruction of the nanotube structure. Pan

et al. [17] reported the attachment of mercaptoacetic acid capped CdSe QD to the surface of MWCNT that had been covalently functionalized with ethylenediamine. The $-NH_2$ moeity on the functionalized MWCNT reacts with the carboxylic acid group on the QD to attach the QD to the MWCNT. Engtrakul et al. [18] reported self-organization of semiconductor InP and CdSe QD on the surface of SWNT. SWNT dispersed in toluene were stirred with tri-n-octylphosphine/tri-n-octylphosphine oxide (TOP/TOPO) ligated QD at 80°C for 18 h under N_2 atmosphere. It was observed that small QD adhere randomly to the SWNTs while the larger ones prefer the long linear chains for self-assembly. Landi et al. [19] have reported noncovalent attachment of CdSe QD to SWNT via the 1-pyrenebutyric acid N-hydroxysuccinimide ester (PBASE) linker. Ligand exchange of TOPO capped CdSe QD with 4-aminothiophenol was performed. Noncovalent coupling of PBASE was indicated by the redshift of the fluorescence peak. Raman spectroscopy indicated that the D and the G bands were unaltered on attachment. Schulz-Drost et al. [20] reported the synthesis of CdTe QD coupled with SWNT. First, CdTe QD stabilized by thioglycolic acid and 2-mercaptoethanesulfonate (MESNA) were synthesized. The thiol groups were proposed to stabilize the QD and the –COOH group of the thioglycolic acid and MESNA ensured solubility in water. Thioglycolic acid enabled covalent attachment to 1-pyrenemethylamine through peptide condensation. The latter was the source of pyrene that was used to π-π stack on the structure of SWNT and acted as a linker between the SWNT and QD. A notable feature in the emission spectra was fourfold quenching and 13 nm redshift of the CdTe peak on attachment to SWNT. Juárez et al. [21] injected CNT suspensions (both SWNT and MWCNT, in different experiments) while synthesizing CdSe by organometallic routes. Substantial coverage of QD was obtained on both SWNT and MWCNT. Current-voltage characteristics were studied on a device constructed by bridging this composite between two gold electrodes on a silica support.

Pan et al. [22] reported attachment of CdSe QD functionalized by –COOH to MWCNT covalently functionalized with –COOH, –OH, and $-NH_2$. For the former two, the attachment was not too effective as indicated by the TEM images, while for the later, the QD were beautifully decorated on the CNT. The authors attributed this to the electrostatic repulsion of the QD–COOH with CNT–COOH and CNT–OH. Quenching of fluorescence of the QD as a function of CNT concentration was studied and the quenching constants were determined from the Stern-Volmer and double logarithmic equations. It was found that the Stern-Volmer constant K_{sv} for the –COOH, –OH, and the $-NH_2$ functionalized CNT was 0.060, 0.106, and 0.176 L/mg, respectively. The higher quenching constant for the latter indicated more effective resonance energy transfer from the QD to the CNT. This is consistent with more effective attachment of the QD to the $-NH_2$ functionalized CNT as compared to the other two. Loscutova and Barron [23] reported coating of CdS and CdSe on SWNT. CNT were introduced into a flask containing cadmium oxide and n-tetradecylphosphine oxide, and this was followed by introduction of selenium-tributylphosphine complex resulting in the formation of QD coated CNT. Two media were used: TOPO (tri-n-octylphosphine oxide) and 1-octadecene. The TEM images were not too well defined; however it should be noted that this was one of the pioneering reports of a CNT-QD composite. Li et al. [15] reported a composite of pyridine capped CdSe nanocrystals on the surface of SWNT. First, the synthesis of TOPO capped CdSe nanocrystals was performed, followed by ligand exchange of TOPO with pyridine. Then CNT deposited on a graphite substrate were dipped into a suspension of pyridine capped QD. Haremza et al. [24] reported the covalent attachment of CdSe nanocrystals onto SWNT. The SWNT were pre-functionalized with acid chloride. This was followed by addition of CdSe stabilized by a bifunctional linker 2-aminoethanethiol. Functionalization of the QD was achieved by ligand exchange of TOPO with 2-aminoethanethiol. The –SH group of 2-aminoethanethiol attaches to the QD while the $-NH_2$ group results in attachment to the acid chloride functionalized SWNT by means of an amide linkage. Dutta et al. [12] reported attachment of ZnO semiconducting QD to MWCNT. The conjugation took place via formation of a micelle of sodium dodecylbenzenesulfonate (SDBS) in a polar solvent.

There have been reports of attachment of PbS-QD to CNTs, but they are far fewer in number. Further, in most of them the size of the QD involved is greater than that required for quantum confinement (10 nm) and the attachment is covalent in nature. Thus, our present report, where the size of the QD is 2.7 nm and the nature of attachment is noncovalent, is quite significant. Henceforth, we refer to particles of sizes much greater than those required for exhibiting quantum confinement as nanoparticles (NP) rather than as QD. Jana et al. [25] reported the growth of PbS NP of average size around 50 nm on the surface of MWCNTs that was covalently functionalized with –COOH group. Wang et al. [13] reported the synthesis of PbS-MWCNT composites by treatment of presynthesized PbS-QD with MWCNT stabilized by oleylamine. The coverage on the surface of MWCNT was manipulated by varying the ratio of PbS to MWCNT. Blueshift (from 1480 nm to 1170 nm) and quenching of the NIR photoluminescence peak in the unwashed sample on addition of the PbS NP to the MWCNT were observed. In the samples that were washed to remove all free PbS-QD, the total quenching of photoluminescence was observed. The quenching of the photoluminescence was attributed to energy transfer from the PbS-QD to the MWCNT while the blueshift was attributed to change in optical properties of the PbS-QD on interaction with the MWCNT. Further, the composites were embedded in a hole conducting polymer, poly(3-hexylthiophene), for optical studies. Fernandes et al. [10] loaded preformed PbS nanoparticles (NP) onto the cavities of MWCNT that were grown on a silica substrate. Photocurrent response of the device so obtained was measured. Yu et al. [16] reported the synthesis of PbS/MWCNT by addition of lead acetate to surfactant cetyltrimethylammoniumbromide (CTAB) treated MWCNT, followed by addition of thioacetamide. The average size of the PbS NP was 20 nm, well beyond the range of quantum confinement. It was observed that the fluorescence intensity

of the peak corresponding to PbS NP in the NIR region is lower in the composite than in pure PbS NP. Our group [26] reported the attachment of PbS-QD to SWNT by noncovalent methods. The QD stabilized by 1,2-BDMT were prepared by previously unreported ultrasound assisted methods and either attached SWNT by noncovalent interactions or were grown in situ on noncovalently functionalized SWNT. Novel methods to attach semiconducting QD to CNT are always important for demonstrating predicted applications as well as exploring new ones. Literature search revealed no reported methods to noncovalently attach PbS-QD smaller than 5 nm to SWNT except our previous report [26]. This current report presents an additional route to attach PbS-QD to CNT that overcomes the problems associated with controlling the morphology and size distribution of the QD encountered in our previous report [26].

2. Experimental Details

PbS-QD of size 2.7 nm stabilized by oleic acid were purchased from Evident Technologies. 1,2-BDMT (95%) was purchased from Sigma Aldrich. SWNT (semiconducting) were purchased from Unidym Carbon Nanotubes, Menlo Park, California. MWCNT were purchased from Nanostructured and Amorphous Materials Inc., Los Alamos, New Mexico. The diameter range for MWCNT was 30–40 nm. Ethanol (95%) was purchased from Pharmaco. All chemicals were used as received without further purification. All TEM micrographs were obtained on a Philips CM 200 FEG HRTEM operating at 200 keV. Copper grids purchased from Ted Pella were carbon coated for use in TEM measurements. The samples were prepared by depositing a 4 μL drop of the solution onto the grid and the solvent evaporated in air. For bath sonication experiments, a Fischer Scientific FS60H bath sonicator with an output of 100 W, 42 kHz (±6%), was used. For tip sonication, a Cole-Palmer CPX 130 tip sonicator, operating at 100W and equipped with a Ti horn, was used. Particle size was determined from TEM micrographs manually by using the "ImageJ" software version 1.44p, a freeware developed by the National Institutes of Health, USA. 1 mg of MWCNT was dispersed in 20 mL ethanol (95%) by bath sonication (MWCNT suspension). 1 mg of SWNT was dispersed in 20 mL ethanol (95%) by tip sonication (SWNT suspension). For tip sonication, a 3 s pulse was used at 80% power, followed by 3 s delay; total time under sonication excluding the delay was 1 h. NIR emission spectra were measured in a 1 cm optical path length quartz cuvette at room temperature using a Horiba Jobin-Yvon Nanolog 916B fluorescence spectrophotometer that was equipped with an IGA 512 InGaAs detector cooled to 77 K using liquid N_2. Five nm slit width was used for both excitation and emission slits. Excitation wavelength was 450 nm. Absorption spectra were obtained by means of a Guided Wave (Rancho Cordova, CA) model LS-E-VIS-NIR spectrometer. The samples were pipetted into a 1 cm optical path length quartz cuvette at room temperature and placed into the sample holder of the spectrometer for measurements. NIR fluorescence and absorbance data were processed using GRAMS 32 software version 5.21 obtained from Galactic Industries Corporation. FTIR spectra were obtained on a Thermo-Nicolet Avatar 370 DTGS IR spectrometer equipped with a smart arc sample holder. Data was processed by EZ Omnic software ver. 7.0 by Thermo Electron Corporation.

1,2-BDMT (30 mg) was dissolved in 1 mL of ethanol (95%) by bath sonication. To this 50 μL of MWCNT suspension was added and the mixture was placed under bath sonication for 30 minutes. The suspension was centrifuged at 14000 rpm for 1 hr followed by decantation. To the residue 500 μL of ethanol was added, and the suspension was placed under bath sonication for ~2 min. Thereafter commercially obtained PbS-QD (10 μL), diluted by addition of 10 μL of the as obtained suspension in 1 mL of tetrachloroethylene, was added and the reaction mixture was placed under bath sonication for 1 hr. The composite dispersion was washed twice with ethanol by centrifugation followed by redispersion in ethanol. An analogous process was adopted for SWNT.

3. Results and Discussion

Several approaches have been adopted to attach QD to CNT as reviewed above. Our group recently demonstrated the attachment of preformed PbS-QD stabilized by 1,2-BDMT to SWNT and MWCNT [26]. The QD of sizes 2.7 and 3.6 nm were prepared by novel ultrasound assisted method using ethanol as a solvent and lead nitrate and sodium sulfide as precursors. However, the coverage of PbS-QD on the CNT was not uniform; there were clumps of QD adhering to the surface of the CNT. This was attributed to the small size of the stabilizer as well as the ability of the stabilizer to π-π stack with itself. To overcome this shortcoming, another approach reported by our group [26] was to grow QD on prefunctionalized CNT. PbS-QD were grown in situ on CNT that was previously noncovalently functionalized with 1,2-BDMT. Though the coverage of the QD on the CNT was much more uniform, the size distribution of the QD was large; as such the size of the QD formed on the surface was much larger (5-6 nm) than if the PbS-QD were synthesized without the CNT support. Controlling of the morphology of QD formed by this method was also difficult. To overcome the shortcomings of both of the above methods, this current work reports a third method: attachment of commercially available oleic acid stabilized monodispersed PbS-QD to the surface of CNT prefunctionalized by an aromatic dithiol. Monodispersed PbS-QD of different sizes that lie within the quantum confinement region, dispersed in toluene and stabilized by oleic acid, are commercially available from Evident Technologies. Thus, the problem of nonuniform size distribution was overcome. The as obtained PbS-QD were characterized by NIR absorbance and fluorescence spectroscopy as well as by TEM. Figures 1 and 2 depict the optical spectra and the TEM micrograph, respectively. Consistent with the size of the QD, they absorb at 997 nm and fluoresce at 1094 nm (Figure 1). The excitation wavelength used for fluorescence studies was 450 nm. Consistent with previous reports, the TEM micrograph shows well-formed and monodispersed QD.

According to the hard-soft-acid base (HSAB) concept, a soft base thiol would stabilize soft PbS better than a hard

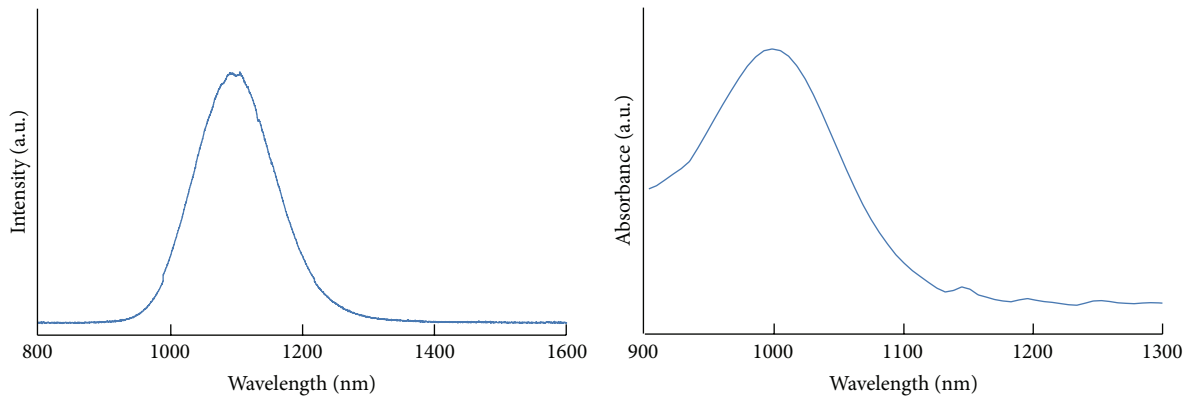

(a) PbS-QD NIR fluorescence spectrum

(b) PbS-QD absorbance spectrum

FIGURE 1: NIR fluorescence (a) and absorbance (b) spectra of the commercially obtained PbS-QD stabilized by oleic acid.

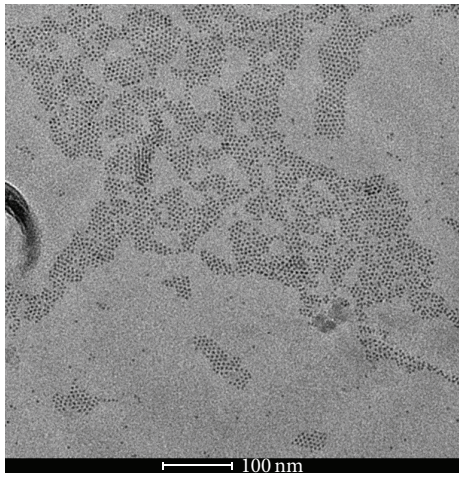

FIGURE 2: TEM micrograph of the commercially obtained PbS-QD stabilized by oleic acid. The scale bar is 100 nm.

base alkyl carboxylate. Exploiting this principle, addition of the commercially obtained PbS-QD stabilized by oleic acid to MWCNT prefunctionalized by 1,2-BDMT is carried out. The aromatic part of the thiol molecules attaches to the CNT framework by π-π stacking interactions and the –SH groups then replace oleic acid on the surface of the PbS-QD. First the CNT were dispersed in 95% ethanol by sonication. For SWNT tip sonication was used and for MWCNT bath sonication was used. The approximate concentration of the CNT in this suspension was 0.05 mg/mL. 50 μL of this suspension was added to 1 mL of a concentrated (30 mg/mL) solution of 1,2-BDMT in ethanol and the mixture was subjected to bath sonication for 30 min. The approximate amount of CNT in the mixture is 2.5 μg, while the amount of 1.2-BDMT is 30 mg. It may be noted that mass-wise the percentage of the aromatic ring in 1,2-BDMT is approximately 47.5%, while the CNT are comprised just of these aromatic moieties. In SWNT it may be assumed that all these aromatic rings are on the surface and have equal probability of getting noncovalently functionalized. In case of MWCNT, a fraction of the aromatic moieties are on the outermost wall and capable of being functionalized noncovalently. Thus the ratio of 1,2-BDMT to CNT in our mixture is quite high and this makes the probability of noncovalent functionalization of the CNT surface quite high. The composite was ultracentrifuged at 14000 rpm for 1 hr to precipitate out the functionalized CNT. It was noted that, on ultracentrifugation, the appearance of the functionalized CNT residue is more "fluffy" than that of a residue of CNT that was processed identically except that no 1,2-BDMT was added. The residue was dispersed in 500 μL of ethanol by bath sonication for about 2 min. Thereafter, the as obtained PbS-QD suspension in toluene was diluted by addition of 10 μL of the suspension to 1 mL of tetrachloroethylene (TCE). 10 μL of this diluted suspension was added to the dispersion of CNT in ethanol and the mixture was placed under bath sonication for 1 hr to yield the composite. Excess PbS-QD were removed by washing twice with ethanol. The TEM images of the composites so obtained are shown in Figures 3 and 4. It is clearly seen that the PbS-QD decorate the CNT and do not form clumps or aggregates. The distance between the QD and the nanotube is governed by the length of the alkyl side chain but clearly lies in the range permitting energy transfer from the QD to the CNT. The amount of PbS-QD added determines the degree of coverage of the PbS-QD. Figure 3(b) shows the procedure carried out in the presence of 50 times more (500 μL of the diluted PbS-QD suspension instead of 10 μL described in the experimental section) PbS-QD. It can be seen that the coverage is more than optimum. Hence the amount of PbS-QD was optimized to obtain a good coverage as shown in Figures 3 and 4.

FTIR spectroscopy was used to further characterize the PbS-CNT composites. Figures 5 and 6, respectively, show the relevant spectra of the PbS-QD composites with MWCNT and SWNT. FTIR spectrum for the PbS-QD is nearly featureless from 1400 to 4000 cm^{-1}. The FTIR spectra of both the PbS-MWCNT and PbS-SWNT composites exhibit similar features. The broad peak around 3330 cm^{-1} arises from ethanol in the suspension as well as the free oleic acid released after it was exchanged on the surface of the QD by the dithiol. The peaks at 2970 and 2880 cm^{-1} may be attributed to the ν-SH modes, arising from the 1,2-BDMT. The SH moieties may be attributed to the free SH on the

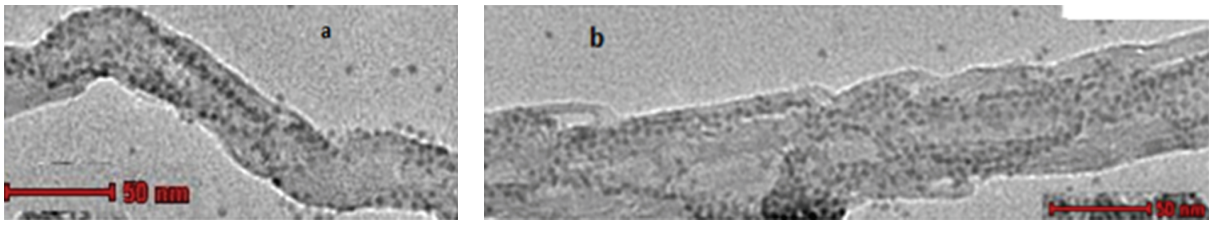

(a) (b)

Figure 3: Commercially obtained PbS-QD attached to thiol functionalized MWCNT by 1,2-BDMT. Scale bar is 50 nm on each.

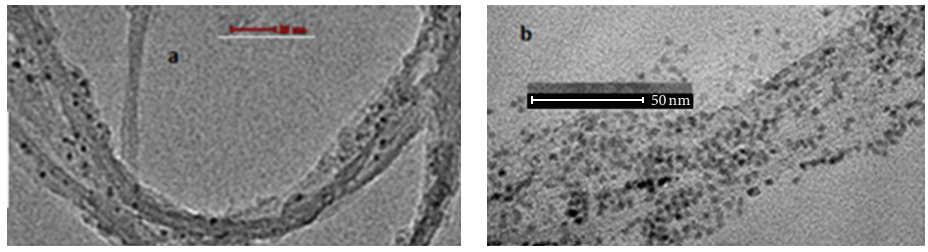

(a) (b)

Figure 4: Attachment of commercially obtained oleic acid stabilized PbS-QD to 1,2-BDMT functionalized SWNT by ligand exchange. (a) depicts results obtained by using quantities of PbS-QD suspension enumerated in the experimental section while (b) shows results of using 50 times more PbS-QD suspension than that enumerated in the experimental section. Scale bar in both (a) and (b) is 50 nm.

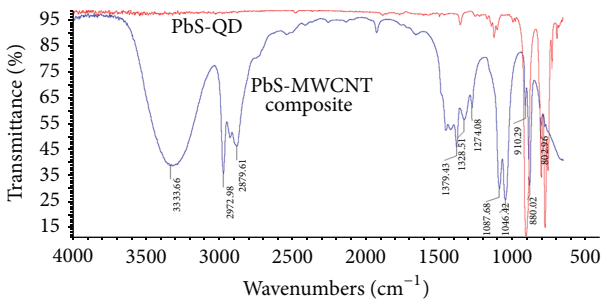

Figure 5: FTIR spectra of PbS-MWCNT composite and PbS-QD.

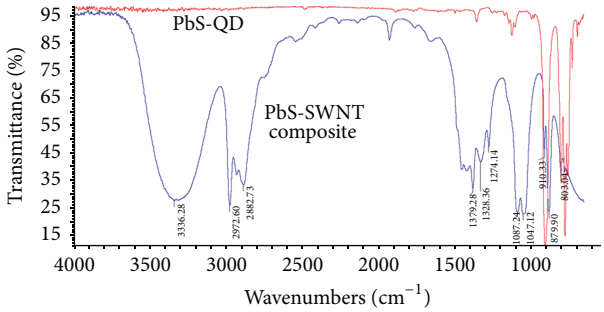

Figure 6: FTIR spectra of PbS-SWNT composite and PbS-QD.

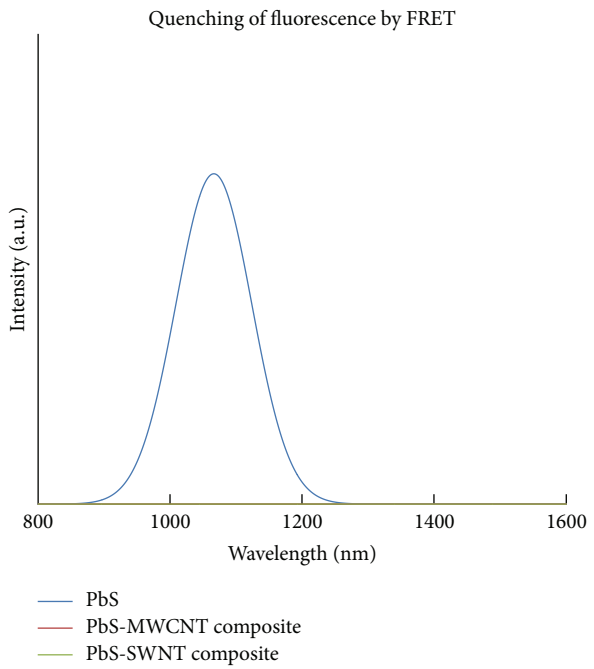

Figure 7: NIR fluorescence spectra of PbS-QD, PbS-MWCNT composite, and PbS-SWNT composite.

1,2-BDMT that do not have a QD attached. Aromatic C=C bending modes are seen from 1500 to 1700 cm^{-1}. These arise from the 1,2-BDMT as well as from the CNT framework. NIR fluorescence spectra of the composites were compared to those of PbS-QD (Figure 7). The suspension of PbS-QD was diluted with ethanol such that the concentration of QD in this suspension was the same as the concentration of QD in either of the composite suspensions. It may be noticed from Figure 7 that a total quenching of NIR fluorescence was observed in the composite suspensions. Föster resonance energy transfer (FRET) is possible from the QD to the CNT if the energy

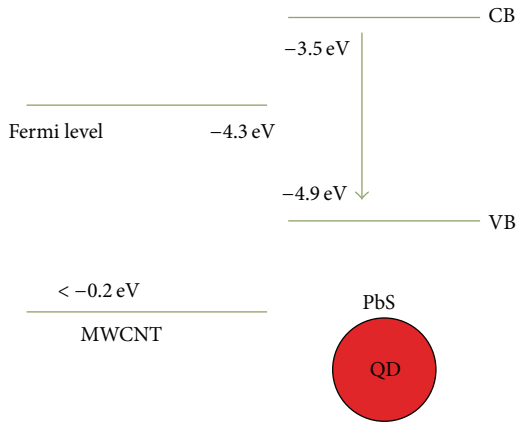

Scheme 1

Scheme 1: Energy levels of MWCNT and PbS NP. The bandgap of the semiconductor QD depends on the size. The smaller PbS-QD have a larger bandgap while the larger PbS-QD have a smaller bandgap. Energy values for PbS NP are based on a size of 20 nm for the particle (from [25]). For the size of PbS-QD used for this work, the VB lies at the same energy level shown, while the CB lies at a much higher level. The energy levels shown are not to scale.

gap is suitable and the two lie closer to the Föster radius. As was previously reported the energy gap for both of the acceptors MWCNT [16] and SWNT [15] is suitable for FRET from PbS-QD (donor). The CNT and the QD, separated by a C–C–S bond, lie closer than the Föster radius of 10 nm. The energy levels are schematically depicted for MWCNT and PbS-QD in Scheme 1. The values for the energy levels for the PbS-QD in Scheme 1 are obtained from the literature [16] for QD of size 20 nm. Since the size of the PbS-QD used here is ~2.7 nm, the conduction band would be much higher in energy. The level of valence band remains the same for all sizes of PbS-QD, while the band gap increases as the size of the QD decreases. For semiconducting SWNT, the corresponding values for conduction and valence bands are at −4.8 eV and −5.4 eV, respectively, and the Fermi level is at −4.4 eV [15]. Quenching of fluorescence of semiconductor QD on attachment to CNT was previously demonstrated for PbS- [11, 16], CdSe [15, 20, 22], ZnO [12], and CdSe-ZnS [27] QD. Though qualitatively quenching the fluorescence of the PbS-QD is demonstrated, a detailed quantitative analysis of the degree of FRET is beyond the scope of this report. It may be noted that though SWNT themselves fluoresce in the NIR region, the individual SWNT have to be unbundled to individual strands by means of dispersion using a surfactant or attachment to a solid support for the fluorescence to be experimentally observed. In this study the SWNT were not unbundled into individual strands; thus fluorescence of the SWNT may be discounted.

As a future direction, molecules bearing a structure similar to 1,2-BDMT could be explored as linkers of the QD to the CNT. The selection of molecules would tailor the separation of the two and would thus influence energy transfer from the former to the latter. As an immediate study to explore potential applications of the composites synthesized in this study, an appropriate device may be constructed as demonstrated by Kamat [5] and incident photon to current generation efficiency (IPCE) studies may be carried out on exposure to wavelengths in the NIR region. Such a study would test the suitability of this composite for use as a component of a solar energy conversion device. The composite may also be tested for biological imaging applications; however the toxicity tests must be carried out before in vivo testing. In the past toxicity of the QD was countered by passivation of the surface with ligands [2].

4. Conclusion

Addition of commercially obtained oleic acid stabilized PbS-QD to CNT prefunctionalized with aromatic thiols results in PbS-QD-CNT composites. This method exploits the thiols' greater affinity to attach to the surface of PbS-QD as compared to oleic acid, enabling exchange of the oleic acid with the thiols on the surface of the QD. The aromatic framework of the thiols attaches to the CNT by π-π stacking interaction thus facilitating the formation of the composites. The composites were characterized by TEM and FTIR. Quenching of NIR fluorescence of the PbS-QD was observed on formation of composites with the CNT. The composites so developed have tremendous potential to be explored as novel materials in the field of solar energy harvesting, biological sensors, and IR detectors.

Conflict of Interests

The authors declare that there is no conflict of interests with any person or entity referred to in this paper. No competing interest exists and professional judgment concerning the validity of research is not influenced by a secondary interest, such as financial gain. The commercial entities referred to in this document such as but not limited to "Sigma-Aldrich" or "Amorphous Materials Inc." merely act as commercial suppliers for raw materials used for experiments and have no affiliation whatsoever with either of the authors.

References

[1] V. I. Klimov, "Mechanisms for photogeneration and recombination of multiexcitons in semiconductor nanocrystals: implications for lasing and solar energy conversion," *Journal of Physical Chemistry B*, vol. 110, no. 34, pp. 16827–16845, 2006.

[2] C. L. Amiot, S. Xu, S. Liang, L. Pan, and J. X. Zhao, "Near-infrared fluorescent materials for sensing of biological targets," *Sensors*, vol. 8, no. 5, pp. 3082–3105, 2008.

[3] S. A. Mcdonald, G. Konstantatos, S. Zhang et al., "Solution-processed PbS quantum dot infrared photodetectors and photovoltaics," *Nature Materials*, vol. 4, no. 2, pp. 138–142, 2005.

[4] J. J. Peterson and T. D. Krauss, "Fluorescence spectroscopy of single lead sulfide quantum dots," *Nano Letters*, vol. 6, no. 3, pp. 510–514, 2006.

[5] P. V. Kamat, "Quantum dot solar cells. Semiconductor nanocrystals as light harvesters," *Journal of Physical Chemistry C*, vol. 112, no. 48, pp. 18737–18753, 2008.

[6] C.-T. Yuan, Y.-G. Wang, K.-Y. Huang et al., "Single-particle studies of band alignment effects on electron transfer dynamics

from semiconductor hetero-nanostructures to single-walled carbon nanotubes," *ACS Nano*, vol. 6, no. 1, pp. 176–182, 2012.

[7] S. Y. Jeong, S. C. Lim, D. J. Bae et al., "Photocurrent of CdSe nanocrystals on single-walled carbon nanotube-field effect transistor," *Applied Physics Letters*, vol. 92, no. 24, Article ID 243103, 2008.

[8] B. J. Landi, S. L. Castro, H. J. Ruf, C. M. Evans, S. G. Bailey, and R. P. Raffaelle, "CdSe quantum dot-single wall carbon nanotube complexes for polymeric solar cells," *Solar Energy Materials and Solar Cells*, vol. 87, no. 1–4, pp. 733–746, 2005.

[9] H.-C. Huang, S. Barua, G. Sharma, S. K. Dey, and K. Rege, "Inorganic nanoparticles for cancer imaging and therapy," *Journal of Controlled Release*, vol. 155, no. 3, pp. 344–357, 2011.

[10] G. E. Fernandes, Z. Liu, J. H. Kim, C.-H. Hsu, M. B. Tzolov, and J. Xu, "Quantum dot/carbon nanotube/silicon double heterojunctions for multi-band room temperature infrared detection," *Nanotechnology*, vol. 21, no. 46, Article ID 465204, 2010.

[11] G. E. Fernandes, M. B. Tzolov, J. H. Kim, Z. Liu, and J. Xu, "Infrared photoresponses from PbS filled multiwall carbon nanotubes," *Journal of Physical Chemistry C*, vol. 114, no. 51, pp. 22703–22709, 2010.

[12] M. Dutta, S. Jana, and D. Basak, "Quenching of photoluminescence in Zno QDs decorating multiwalled carbon nanotubes," *ChemPhysChem*, vol. 11, no. 8, pp. 1774–1779, 2010.

[13] D. Wang, J. K. Baral, H. Zhao et al., "Controlled fabrication of pbs quantum-dot/carbon-nanotube nanoarchitecture and its significant contribution to near-infrared photon-to-current conversion," *Advanced Functional Materials*, vol. 21, no. 21, pp. 4010–4018, 2011.

[14] A. L. Rogach, T. A. Klar, J. M. Lupton, A. Meijerink, and J. Feldmann, "Energy transfer with semiconductor nanocrystals," *Journal of Materials Chemistry*, vol. 19, no. 9, pp. 1208–1221, 2009.

[15] Q. Li, B. Sun, I. A. Kinloch, D. Zhi, H. Sirringhaus, and A. H. Windle, "Enhanced self-assembly of pyridine-capped CdSe nanocrystals on individual single-walled carbon nanotubes," *Chemistry of Materials*, vol. 18, no. 1, pp. 164–168, 2006.

[16] D. Yu, Y. Chen, B. Li, X. Chen, and M. Zhang, "Fabrication and characterization of PbS/multiwalled carbon nanotube heterostructures," *Applied Physics Letters*, vol. 90, no. 16, Article ID 161103, 2007.

[17] B. Pan, D. Cui, R. He, F. Gao, and Y. Zhang, "Covalent attachment of quantum dot on carbon nanotubes," *Chemical Physics Letters*, vol. 417, no. 4-6, pp. 419–424, 2006.

[18] C. Engtrakul, Y.-H. Kim, J. M. Nedeljković et al., "Self-assembly of linear arrays of semiconductor nanoparticles on carbon single-walled nanotubes," *Journal of Physical Chemistry B*, vol. 110, no. 50, pp. 25153–25157, 2006.

[19] B. J. Landi, C. M. Evans, J. J. Worman, S. L. Castro, S. G. Bailey, and R. P. Raffaelle, "Noncovalent attachment of CdSe quantum dots to single wall carbon nanotubes," *Materials Letters*, vol. 60, no. 29-30, pp. 3502–3506, 2006.

[20] C. Schulz-Drost, V. Sgobba, C. Gerhards et al., "Innovative inorganic-organic nanohybrid materials: coupling quantum dots to carbon nanotubes," *Angewandte Chemie International Edition*, vol. 49, no. 36, pp. 6425–6429, 2010.

[21] B. H. Juárez, C. Klinke, A. Kornowski, and H. Weller, "Quantum dot attachment and morphology control by carbon nanotubes," *Nano Letters*, vol. 7, no. 12, pp. 3564–3568, 2007.

[22] B. Pan, D. Cui, C. S. Ozkan et al., "Effects of carbon nanotubes on photoluminescence properties of quantum dots," *Journal of Physical Chemistry C*, vol. 112, no. 4, pp. 939–944, 2008.

[23] R. Loscutova and A. R. Barron, "Coating single-walled carbon nanotubes with cadmium chalcogenides," *Journal of Materials Chemistry*, vol. 15, no. 40, pp. 4346–4353, 2005.

[24] J. M. Haremza, M. A. Hahn, T. D. Krauss, S. Chen, and J. Calcines, "Attachment of single CdSe nanocrystals to individual single-walled carbon nanotubes," *Nano Letters*, vol. 2, no. 11, pp. 1253–1258, 2002.

[25] S. Jana, D. Banerjee, A. Jha, and K. K. Chattopadhyay, "Fabrication of PbS nanoparticle coated amorphous carbon nanotubes: structural, thermal and field emission properties," *Materials Research Bulletin*, vol. 46, no. 10, pp. 1659–1664, 2011.

[26] A. Das and C. M. Wai, "Ultrasound-assisted synthesis of PbS quantum dots stabilized by 1, 2-benzenedimethanethiol and attachment to single-walled carbon nanotubes," *Ultrasonics Sonochemistry*, vol. 21, pp. 892–900, 2014.

[27] V. Biju, T. Itoh, Y. Baba, and M. Ishikawa, "Quenching of photoluminescence in conjugates of quantum dots and single-walled carbon nanotube," *Journal of Physical Chemistry B*, vol. 110, no. 51, pp. 26068–26074, 2006.